AECL-8271

ATOMIC ENERGY OF CANADA LIMITED

L'ÉNERGIE ATOMIQUE DU CANADA LIMITÉE

PREDICTED AND MEASURED VELOCITY DISTRIBUTIONS IN A MODEL HEAT EXCHANGER

Répartitions prédites et mesurées des vitesses dans un modèle d'échangeur de chaleur

by

D.B. RHODES and L.N. CARLUCCI

Paper presented at the 1983 CNS/ANS International Conference on Numerical Methods in Nuclear Engineering, Montreal, September 6-9.

Chalk River Nuclear Laboratories Laboratoires nucléaires de Chalk River

Chalk River, Ontario

January 1984 janvier

ATOMIC ENERGY OF CANADA LIMITED

PREDICTED AND MEASURED VELOCITY DISTRIBUTIONS IN A MODEL HEAT EXCHANGER

by

D.B. Rhodes and L.N. Carlucci

Paper presented at the 1983 CNS/ANS International Conference on Numerical Methods in Nuclear Engineering, Montreal, September 6-9.

Engineering Research Branch
Special Projects Division
Chalk River Nuclear Laboratories
Chalk River, Ontario K0J 1J0
1984 January

AECL-8271

L'ENERGIE ATOMIQUE DU CANADA, LIMITEE

Répartitions prédites et mesurées des vitesses dans un modèle d'échangeur de chaleur

par

D.B. Rhodes et L.N. Carlucci

Résumé

Les prédictions numériques faites au moyen d'un concept de milieux poreux sont comparées, dans ce rapport, aux mesures effectuées dans un modèle d'échangeur de chaleur en ce qui concerne la répartition bidimensionnelle, isotherme et latérale des vitesses. Les calculs et les mesures ont été effectués avec et sans tubes présents dans le modèle. L'effet des fuites entre tubes et chicanes a également été étudié. La comparaison a été effectuée pour valider certains concepts de milieux poreux employés dans un code machine actuellement développé pour prédire en détail l'écoulement du côté de la gaine dans une vaste gamme de géométries pour les tubes en gaine des échangeurs de chaleur.

Rapport présenté au congrès international 1983 de la Société nucléaire canadienne et de ANS (American Nuclear Society) sur les méthodes numériques employées en génie nucléaire, tenu à Montréal du 6 au 9 septembre 1983.

Département de recherche en ingénierie
Laboratoires nucléaires de Chalk River
Chalk River, Ontario K0J 1J0

Janvier 1984

AECL-8271

ATOMIC ENERGY OF CANADA LIMITED

PREDICTED AND MEASURED VELOCITY DISTRIBUTIONS IN A MODEL HEAT EXCHANGER

by

D.B. Rhodes and L.N. Carlucci

ABSTRACT

This paper presents a comparison between numerical predictions, using the porous media concept, and measurements of the two-dimensional isothermal shell-side velocity distributions in a model heat exchanger. Computations and measurements were done with and without tubes present in the model. The effect of tube-to-baffle leakage was also investigated. The comparison was made to validate certain porous media concepts used in a computer code being developed to predict the detailed shell-side flow in a wide range of shell-and-tube heat exchanger geometries.

Paper presented at the 1983 CNS/ANS International Conference on Numerical Methods in Nuclear Engineering, Montreal, September 6-9.

Engineering Research Branch
Chalk River Nuclear Laboratories
Chalk River, Ontario KOJ 1J0
1984 January

AECL-8271

PREDICTED AND MEASURED VELOCITY DISTRIBUTIONS

IN A MODEL HEAT EXCHANGER

D.B. Rhodes and L.N. Carlucci

Atomic Energy of Canada Limited
Chalk River Nuclear Laboratories
Chalk River, Ontario
K0J 1J0

NOMENCLATURE

a	Convection-diffusion coefficent in finite control volume equation
c	Radial tube-to-baffle clearance
C_μ	Constant in turbulence model = 0.09
d	Tube diameter = 1.27 cm
f	Friction factor
K	Loss coefficient
k	Turbulence kinetic energy
ℓ	Length scale
P,P'	Pressure and pressure correction
p	Tube pitch = 1.91 cm
Su	Source term in finite control volume equation

Re	Reynolds number
t	Baffle thickness
u,v	Velocity in x and y direction
x,y	Cartesian coordinates
β	Local volume porosity = fluid volume÷total volume
ε	Turbulence kinetic energy dissipation rate
μ	Dynamic viscosity
ρ	Density
ϕ	General transport parameter in finite control volume equation, stands for u,v,P',k or ε

Subscripts

b	baffle
c	cross-flow
eff	Effective
h	hydraulic
m	Measured
nb	Neighbouring point node
p	Parallel-flow, main node point
t	tube, turbulent
u,v	u and v velocities

1. INTRODUCTION

Tube failures due to corrosion, fatigue or fretting-wear in nuclear shell-and-tube heat transfer equipment can result in costly station shut-downs and, in some cases, radiation exposure to maintenance personnel. An a priori knowledge of the detailed shell-side flow and heat transfer could prove useful in identifying problem areas such as stagnant corrosion-prone and high velocity vibration-prone zones. Corrective measures could then be taken to avoid potential tube damage.

A computer code to predict the detailed shell-side flow and heat transfer in a wide range of shell-and-tube heat exchanger geometries is being developed [1]. The code employs porous media principles to account for the flow volume reduction and for the distributed hydraulic and thermal resistance of tube bundles, baffles and other internal obstacles [2,3]. Because empirical correlations are used to characterize the distributed resistance, it is important to validate code predictions with experimental measurement. This paper presents a comparison between numerical predictions and measurements [4] of two-dimensional isothermal velocity distributions in a model heat exchanger. To assess the efficacy of the porous media theory, computations and measurements were done with and without tubes present, as well as with and without tube-to-baffle leakage in the model heat exchanger.

2. CONSERVATION EQUATIONS

The equations governing the steady two-dimensional isothermal turbulent flow of an incompressible fluid in a porous medium are those of momentum and continuity. Using the Boussinesq eddy viscosity concept to model Reynolds stresses [5], these equations take on the following conservation forms in cartesian co-ordinates,

x-momentum:

$$\frac{\partial}{\partial x}\left[\beta\left(\rho u^2-\mu_{eff}\frac{\partial u}{\partial x}\right)\right]+\frac{\partial}{\partial y}\left[\beta\left(\rho uv-\mu_{eff}\frac{\partial u}{\partial y}\right)\right]$$

$$=\frac{\partial}{\partial x}\left(\beta\mu_{eff}\frac{\partial u}{\partial x}\right)+\frac{\partial}{\partial y}\left(\beta\mu_{eff}\frac{\partial v}{\partial x}\right)-\beta\frac{\partial P}{\partial x}-K_u\,\beta\rho|u|u \qquad \ldots(1)$$

y-momentum:

$$\frac{\partial}{\partial x}\left[\beta\left(\rho uv-\mu_{eff}\frac{\partial v}{\partial x}\right)\right]+\frac{\partial}{\partial y}\left[\beta\left(\rho v^2-\mu_{eff}\frac{\partial v}{\partial y}\right)\right]$$

$$=\frac{\partial}{\partial x}\left(\beta\mu_{eff}\frac{\partial u}{\partial y}\right)+\frac{\partial}{\partial y}\left(\beta\mu_{eff}\frac{\partial v}{\partial y}\right)-\beta\frac{\partial P}{\partial y}-K_v\beta\rho|v|v \qquad \ldots(2)$$

continuity:

$$\frac{\partial}{\partial x}(\beta\rho u)+\frac{\partial}{\partial y}(\beta\rho v)=0 \qquad \ldots(3)$$

The porosity, which accounts for the flow volume reduction due to the tube bundle, is assumed to be locally isotropic. Hence if a control volume is entirely within a tube-filled region the corresponding surface permeabilities* and porosity are numerically equal and independent of direction. Thus, the porosity within the tube bundle

---

*Surface permeability=ratio of fluid area to fluid-plus-solid area on a control volume face.

is a constant calculated from the characteristic pitch and tube diameter. In the present work, the tube bundle is laid out in a non-equilateral triangular pattern (Figure 1) so that its porosity is given by:

$$\beta_t = 1 - \frac{\pi}{4} \left(\frac{d}{p} \right)^2 \qquad \ldots(4)$$

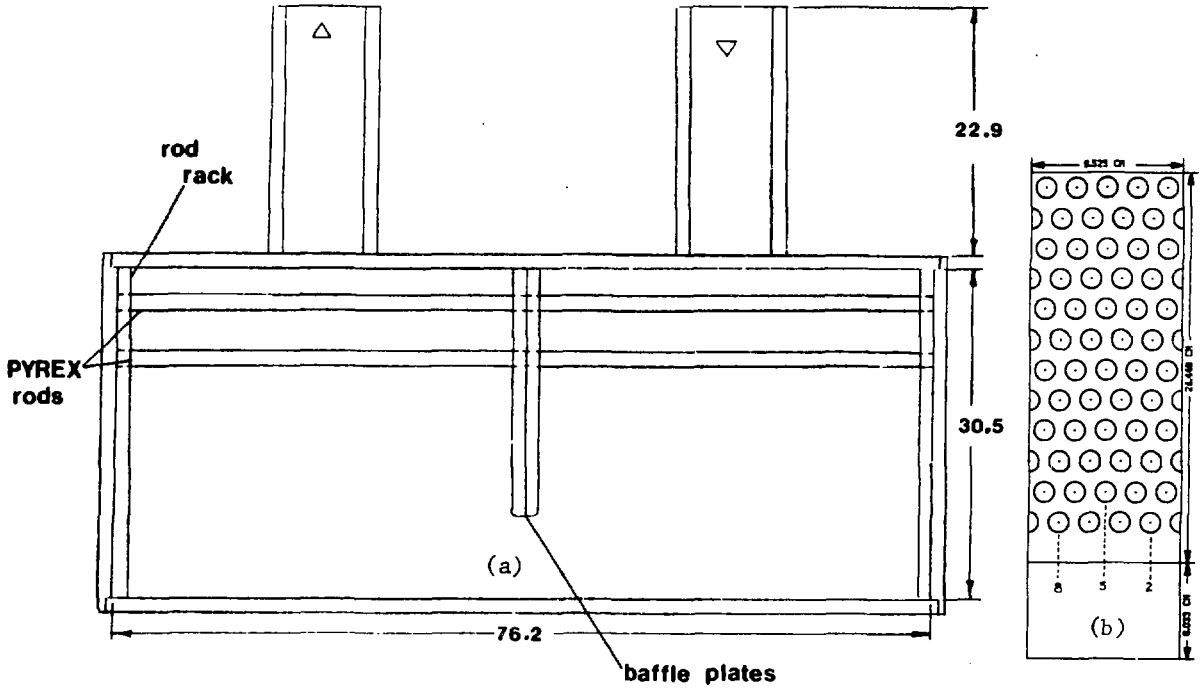

FIGURE 1: Heat Exchanger Model-(a) Front View, (b) End View Showing the Three Measuring Planes 2,5 and 8.

2.1 Hydraulic Impedances

The coefficients K_u and K_v in the momentum equations reflect the local hydraulic resistance due to the tubes and/or baffle. They are defined by:

$$K_u = 2\left(\frac{f_p}{d_h}\right)\left[\frac{1-\beta}{1-\beta_t}\right] + \frac{K_b}{\Delta x} \qquad \ldots(5)$$

$$K_v = \left(\frac{2f_c}{p}\right)\left(\frac{p\beta}{p-d}\right)^2\left[\frac{1-\beta}{1-\beta_t}\right] \qquad \ldots(6)$$

where, for the configuration being studied, the parallel flow friction factor is calculated from [3]:

$$f_p = \begin{cases} 31/Re_p; & Re_p < 2250 \\ 0.131\ Re_p^{-0.294}; & 2250 \leq Re_p < 25000 \\ 0.066\ Re_p^{-0.227}; & Re_p \geq 25000 \end{cases} \qquad \ldots(7)$$

the cross-flow friction factor is given by [6]:

$$f_c = \begin{cases} 0.619\ Re_c^{-0.198}; & Re_c < 8000 \\ 1.156\ Re_c^{-0.2647}; & 8000 \leq Re_c < 200000 \end{cases} \qquad \ldots(8)$$

and the baffle loss coefficient, which consists of shock and frictional Reynolds number-dependent components*, is calculated from:

$$K_b = \begin{cases} 1.92 + \dfrac{7.75\ t}{c\ Re_b}; & \text{baffle-filled region with tube-to-baffle clearance} \\ \infty; & \text{baffle-filled region with no tube-to-baffle clearance} \\ 0; & \text{baffle-free region} \end{cases} \qquad \ldots(9)$$

---

*The tube-to-baffle clearances are modelled as long orifices with the shock or area change component estimated assuming turbulent flow contraction and laminar flow expansion and the frictional component calculated assuming laminar flow in a non-concentric annular passage. Laminar flow in the baffle-to-tube clearance spaces was postulated from preliminary estimates of the Reynolds number over the range of predicted and measured leakage rates. Some computations were also done assuming turbulent flow (Section 6.2).

2.2 Turbulence Model

The effective viscosity is defined as the sum of the laminar and turbulent values:

$$\mu_{eff} = \mu + \mu_t \qquad \ldots(10)$$

For all tube-free model simulations, the turbulence viscosity is calculated on a local basis from the well known k-ε turbulence model [5]:

$$\mu_t = C_\mu \rho k^2 / \varepsilon \qquad \ldots(11)$$

where k and ε are transport parameters calculated by solving two auxiliary partial differential equations. For all tube-filled model simulations, μ_t is assumed constant throughout and is estimated from:

$$\mu_t \simeq C_\mu \rho k_m^{\frac{1}{2}} \ell \qquad \ldots(12)$$

where k_m is a representative measured turbulence intensity [3] and ℓ is an average length scale calculated from:

$$\ell = \frac{1}{2} (2p - d) \qquad \ldots(13)$$

Because the grid used is too coarse to resolve the near-wall flow, the wall shear is estimated using the universal velocity law of the wall [5]. This is done for all tube-filled and tube-free model simulations. For the same reason, near-wall values of k and ε in all tube-free model simulations are estimated using specially-defined wall functions [5].

2.3 Boundary Conditions

All simulations were done with a uniform v-velocity imposed at the model inlet (Figure 1). The v-velocities at the outlet were allowed to vary according to the nearest upstream values but magnitudes were adjusted to satisfy the condition that total outflow equals total inflow.

3. FINITE CONTROL VOLUME DISCRETIZATION AND SOLUTION

3.1 Discretization

The governing equations, including the two auxiliary equations, are discretized using a finite control volume (FCV) method [7], which

is briefly described as follows. The region to be modelled is first subdivided into a number of control volumes overlaid on a non-uniform cartesian grid. A staggered mesh is used so that three different control volumes are associated with a given grid node point, two for the vector variables u and v and one for all remaining scalar variables. Following this, each equation is integrated over its own control volume. The resulting convection-diffusion flux terms at control volume faces are then approximated using the hybrid upwind/central discretization scheme [7]. The FCV equations that result can be cast into the general form:

$$a_p \phi_p = \sum_{nb} a_{nb} \phi_{nb} + Su \qquad \ldots(14)$$

Su is a catch-all term which contains all remaining terms not fitting the standard form. For instance, in the case of momentum, it contains pressure gradient, hydraulic resistance and diffusion terms (see equations (1) and (2)).

Equation (14) is the FCV analogue for all but the continuity equation. Because the FCV equations are solved sequentially by iteration, the momentum equations are always solved on the basis of a guessed pressure field. Thus, in order for the calculated velocity field to satisfy the continuity equation, the pressure and velocity fields must be adjusted. This is done for pressure corrections by combining the momentum and continuity equations into a single equation which has the same form as equation (14). The solution of this equation yields pressure-linked velocity corrections that satisfy continuity, and a pressure field that better satisfies the momentum equation [7].

3.2 Solution

The FCV equations (14) are solved sequentially by employing multiple sweeps of the tridiagonal matrix algorithm (TDMA) line solver. The basic solution process is summarized as follows:

1. Initialize all dependent variables using the correct conditions on the boundary and rough guesses within the modelled region.

2. Assemble the coefficients for the x-momentum equation and solve using the TDMA.

3. Repeat 2 for the y-momentum equation.

4. Set up and solve the pressure correction equation. Use the resulting pressure corrections to correct the velocity and pressure fields.

5. Set up and solve the turbulent kinetic energy equation.

6. Set up and solve the turbulent kinetic energy dissipation equation.

7. Update the turbulent viscosity using equation (11).

8. Repeat steps 2 to 7 until a satisfactory level of convergence is obtained*.

4. HEAT EXCHANGER MODEL

The heat exchanger model [4], shown in Figure 1, consists of a rectangular plexiglas shell containing a vertical baffle and horizontal glass rods arranged in a triangular pattern. The region below the baffle is free of tubes.

Two different drilled baffles were used for the tube-filled model tests, one with holes the same diameter as the tubes to eliminate tube-to-baffle leakage, the other with holes approximately 0.64 mm larger than the tube diameter to simulate typical tube-to-baffle clearances in real heat exchangers. The baffle used for the tube-free model tests was a solid plexiglas plate having the same dimensions as the drilled baffles.

The model was designed to give a two-dimensional shell-side flow field by extending the inlet and outlet the full depth of the shell and by using half rods on the front and back walls to maintain the triangular tube pattern.

Velocities in the model were measured using laser-doppler velocimetry [4]. To permit unimpeded measurement of velocity anywhere in the model, the refractive index of the fluid, a mixture of varsol and xylene, was carefully matched to that of the glass rods. This was achieved by maintaining the mixture fluid temperature to within 0.5°C. For the case with the tubes removed, water was used as a fluid since there was no need for refractive index matching.

Measurements of u and v gap velocities were made in the three planes shown in Figure 1b. All computation results were compared against measurements made in the central plane. Some comparisons were also made between measurements in the front, central, and back planes in the tube-free model and in the tube-filled model with no baffle leakage.

*Note that steps 5 to 7 are executed only for the tube-free model simulations where solutions of the $k-\varepsilon$ equations are required.

5. NUMERICAL SIMULATION

5.1 Simulation Cases

The various simulations that were carried out are described in the table below.

RUN NO.	GRID	MODEL	BAFFLE	FLOW RATE (ℓ/s)	EFFECTIVE VISCOSITY (kg/m/s)
1	C	T	NL	6	0.4
2	F	T	NL	6	0.4
3	C	T	NL	2	0.1
4	C	T	L	6	0.4
5	C	NT	NL	6	V
6	F	NT	NL	6	V

C=Coarse T=Tube-filled NL=No Leakage V=Variable
F=Fine NT=Tube-Free L=Leakage (k-ε Model)

5.2 Grid and Convergence

The basic grid used for the simulation was 36-horizontal by 19-vertical. To test the grid-independence of the solutions, a 98 x 44 grid was also used for two cases. Computing time per iteration on a CDC CYBER 170, Model 175 computer using the basic grid was 0.4 seconds for the constant eddy-viscosity cases and 0.7 seconds for the variable eddy-viscosity cases, for which the two auxiliary turbulence model equations were solved. When the finer grid was used, corresponding computing times were 2.5 and 4.2 seconds per iteration.

Satisfactory convergence was obtained in 50 iterations with the eddy viscosity set to a constant, and in 100 iterations using the k-ε model. The solution was judged to have converged when momentum and mass imbalance residuals were less than 0.1% of typical magnitudes within the model.

6. RESULTS AND DISCUSSION

6.1 Tube-Filled Model With No-Leak Baffle

Figure 2 shows that the predicted and measured velocities for the tube-filled model are generally in good agreement. The inlet jet

spreads quickly, so that the flow is practically uniform by the sixth row of tubes, which corresponds to the third row of arrows in the figure. The low-velocity recirculating zone in the outlet compartment near the bottom of the baffle is accurately simulated. The two small eddies observed in the upper corners of the inlet compartment are also well predicted (Figure 2c).

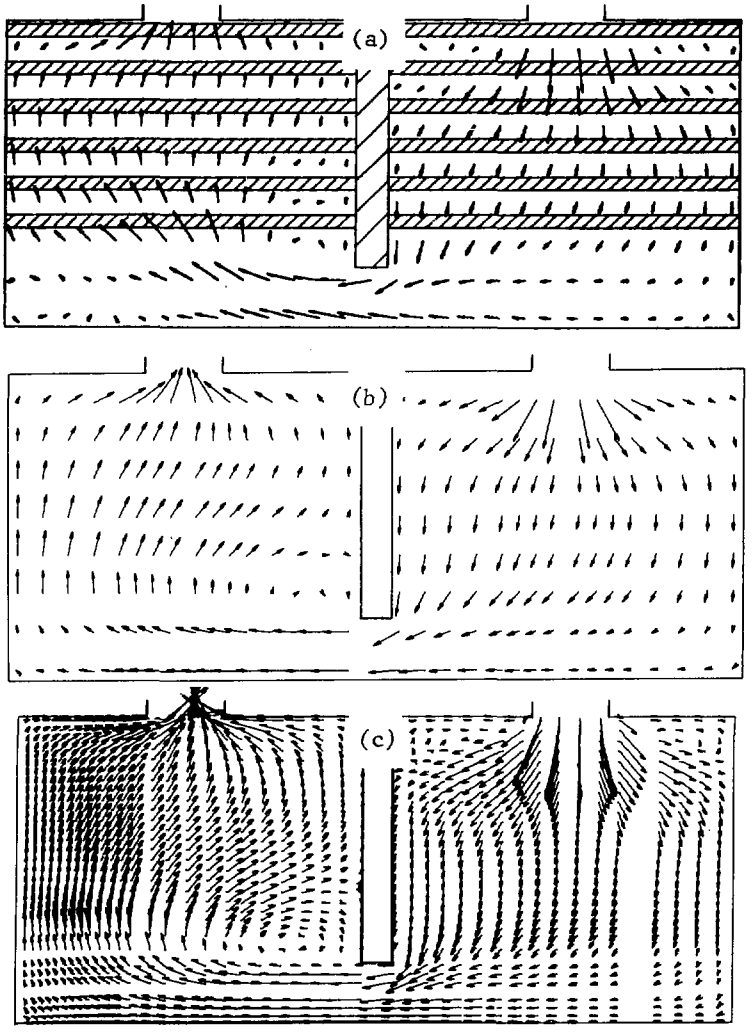

Figure 2: Velocity Distributions for the Tube-Filled Model With No-Leak Baffle-(a) Measured, (b) Coarse Grid Prediction, (c) Fine Grid Prediction; 1 cm=2.25 m/s in All Plots

It is interesting to note that the momentum below the baffle is dissipated more quickly in the model than in the simulation. This is illustrated by the turning of the flow into the tube bundle at approximately mid-span in the model and near the end of the span in the simulation. This discrepancy was observed with both coarse and fine grid simulations, hence it is not considered a resolution problem. It is speculated that the differences between measurement and prediction in this region may be due to three-dimensional effects in the physical model. Close inspection of the velocity measurements in the three planes revealed the presence of a pair of eddies in the lower left corner. It is possible that these eddies account for the apparent loss of momentum of the flow in the physical model, which cannot be modelled with a two-dimensional simulation.

The measured and predicted velocity distributions for the low-flow case were almost the same as those for the higher inlet flow, except that the magnitudes differed by a factor of three. This is not surprising since the flow in both cases is turbulent and the Reynolds numbers only differ by a factor of three.

6.2 Tube-to-Baffle Leakage

A comparison between Figures 2 and 3 indicates that the measured and predicted overall flow pattern remains essentially unchanged when a leaky baffle is introduced. This suggests that the leak rate is a relatively small fraction of the total flow rate.

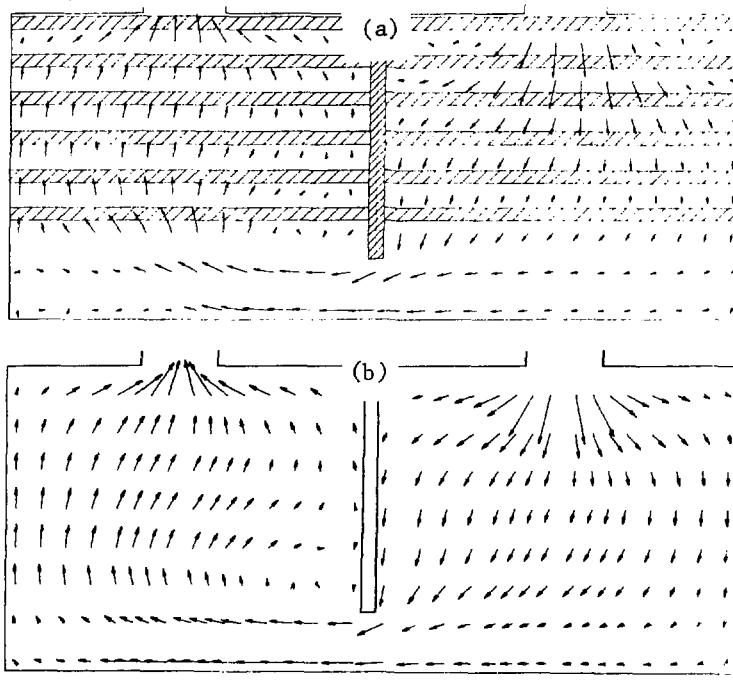

FIGURE 3: Velocity Distributions for the Tube-Filled Model With Tube-to-Baffle Leakage-(a) Measured, (b) Predicted

The predicted leak rate was 0.5 ℓ/s or 8% of the total flow, while the estimated model leak rate was twice this amount. In an attempt to account for this discrepancy, several formulations of the baffle loss coefficient were developed. These were based on various assumptions about the clearance geometry (concentric or non-concentric and flow regime (laminar or turbulent). The implementation of these formulations resulted in a maximum predicted leak rate of 0.6 ℓ/s or 10% of the inlet flow. This is still far short of the 1ℓ/s estimated from measurements. It was eventually concluded that the discrepancy was probably due to the method used to estimate the leak rate from velocity measurements. The estimate was made by taking the average of only two horizontal velocity measurements in the baffle window, multiplying by the window area to get the window flow and subtracting this amount from the inlet flow to estimate the baffle leak rate. A 10% error in estimating the baffle window flow by this procedure is quite likely and could fully account for a 0.5 ℓ/s error in the estimated leak rate.

6.3 Tube-Free Model

The numerical simulation gives a good prediction of the flow in the model with the tubes removed. As shown in Figure 4, the inlet jet is not dispersed as quickly as when tubes are present, but instead flows directly towards the baffle window, inducing large recirculation zones on either side of it. In the outlet compartment, there is one major recirculating zone instead of the predominantly upwards flow with tubes present. The centres of the three large eddies are accurately predicted by both the coarse and fine grid simulations.

Figure 4(b) indicates that in the coarse-grid simulation, the momentum in the lower left corner is not diffused as quickly as in the model. This discrepancy is eliminated when a finer grid is used indicating that it resulted from false diffusion associated with the coarser grid.

7. CONCLUDING REMARKS

This study demonstrates the validity of the porous media principles that account for the presence of tubes and other obstacles by the use of volume-based porosities and distributed resistances. Possible problems in measuring and predicting tube-to-baffle leakage flow have been highlighted. Finally, this study illustrates the feasibility of performing detailed numerical analyses of the flow in actual heat exchangers.

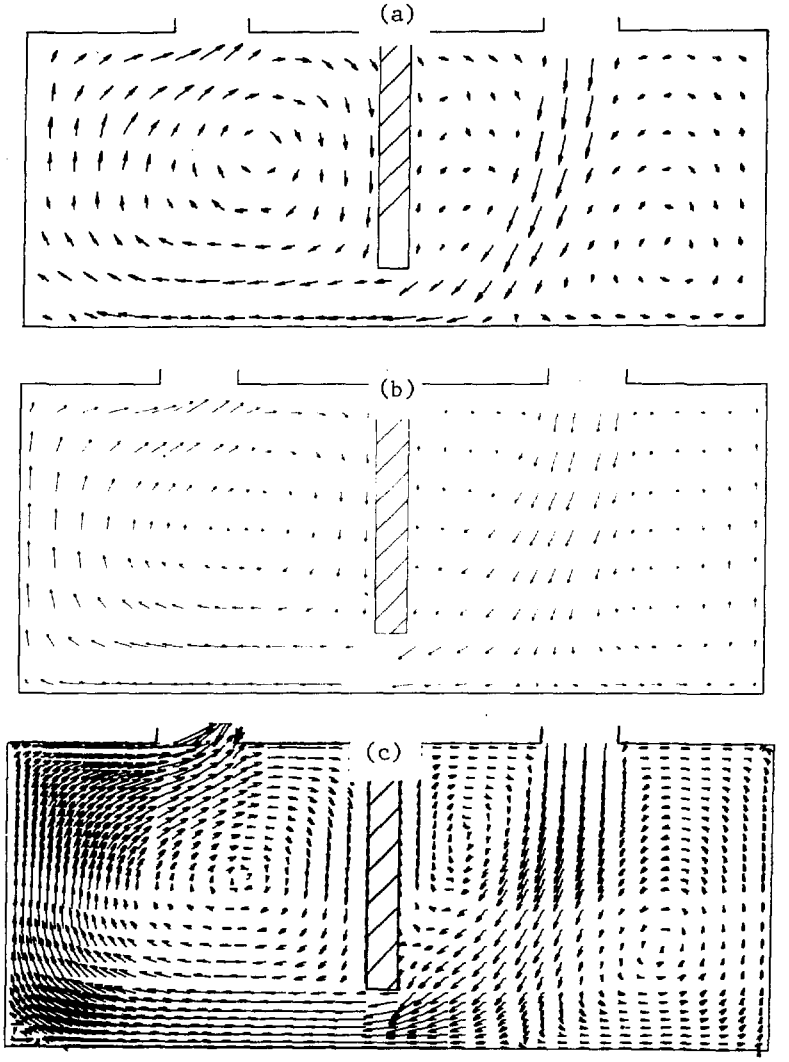

FIGURE 4: Velocity Distributions For The Tube-Free Model-(a)Measured, (b) Coarse Grid Prediction, (c) Fine Grid Prediction

ACKNOWLEDGEMENTS

The experimental work was carried out at the University of Toronto LDA Laboratory by I. Elphick under the supervision of W.W. Martin and I.G. Currie. Their contribution is gratefully acknowledged. Thanks are also due to Ms. J. Thur for typing the manuscript.

REFERENCES

1. Pettigrew, M.J., et al. "Computer Techniques to Analyse Tube-in-Shell Heat Exchangers", Paper prepared for presentation at the 21st AIChE/ASME National Heat Transfer Conference, Seattle, Washington, July 24-27, 1983.

2. Patankar, S.V., Spalding, D.B., "A Calculation Procedure for the Transient and Steady-State Behaviour of Shell-and-Tube Heat Exchangers", Chapter 7 in Heat Exchangers: Design and Theory Sourcebook, Hemisphere Publishing Corp., 1974.

3. Carver, M.B., Carlucci, L.N., Inch, W.R., "Thermal-Hydraulics in Recirculating Steam Generators, THIRST Code User's Manual" AECL-7254, April 1981.

4. Elphick, I.G., "Measurement of Flow Velocities in a Heat Exchanger Model Using LDA", Master's Thesis, University of Toronto, 1981.

5. Rodi, W., "Turbulence Models for Environmental Problems", Chapter in Prediction Methods for Turbulent Flows, ed. by Kollmann, W., Hemisphere Publishing Corp., 1980.

6. Zukauskas, A., "Heat Transfer From Tubes in Cross-Flow" in Advances in Heat Transfer, Volume 8, 1972.

7. Patankar, S.V., Numerical Heat Transfer and Fluid Flow, Hemisphere Publishing Corp., 1980.

ISSN 0067 - 0367

To identify individual documents in the series we have assigned an AECL- number to each.

Please refer to the AECL- number when requesting additional copies of this document

from

Scientific Document Distribution Office
Atomic Energy of Canada Limited
Chalk River, Ontario, Canada
K0J 1J0

Price $2.00 per copy

ISSN 0067 - 0367

Pour identifier les rapports individuels faisant partie de cette série nous avons assigné un numéro AECL- à chacun.

Veuillez faire mention du numéro AECL- si vous demandez d'autres exemplaires de ce rapport

au

Service de Distribution des Documents Officiels
L'Energie Atomique du Canada Limitée
Chalk River, Ontario, Canada
K0J 1J0

Prix $2.00 par exemplaire

241–84